ACS OMEGA

http://pubs.acs.org/journal/acsodf

Article

Carbyne Ring Activated Using $ZnCl_2$ for Hydrogen Adsorption: DFT Study

Luis Alberto Desales Guzmán,* Juan Horacio Pacheco Sánchez, and Juan Salvador Arellano Peraza

Cite This: *ACS Omega* 2022, 7, 10100−10114

Read Online

ACCESS | Metrics & More | Article Recommendations | Supporting Information

ABSTRACT: We have studied the feasibility of activated carbyne as a good hydrogen storage material. Density functional theory (DFT) simulations through van der Waals interactions have been applied to investigate calcium sorption on activating carbyne with zinc dichloride ($ZnCl_2$) and also interactions of molecular hydrogen with pristine carbyne and Ca functionalized on an activated carbyne C_{12}-ring. The obtained results showed that (i) the chemical activation of the C_{12}-ring with $ZnCl_2$ increases its area by 5.17% with respect to pristine carbyne. (ii) Ca atoms at small concentrations tend to get atomically sparse on carbyne, donating +0.94e and +1.05e to the ring, according to Mulliken population analysis and the electrostatic potential fitting charges, respectively. Furthermore, in the presence of calcium, hydrogen sorption increases by 21.8% in comparison with Ca-decorated pure carbyne. (iii) Seven hydrogen molecules per Ca atom have adsorption energy close to the range of ∼0.3−0.5 eV per H_2, which is necessary for effective charge/discharge cycles. (iv) Theoretical uptake (7.11 wt %) with a single Ca atom is higher than the U.S. Department of Energy target (5.5 wt %). Therefore, an activated C_{12}-ring can bind three Ca atoms with its seven H_2 molecules reaching 13.8 wt %. (v) Equilibrium pressure for CaC_{12}−$7H_2$ and Ca_3C_{12}−$21H_2$ systems (5−15 MPa) by means of adsorption isotherm calculations. The calculated van't Hoff desorption temperatures exceed considerably the boiling point of liquid nitrogen. In addition, we also performed DFT-based molecular dynamics simulations for the C_{12}, CaC_{12}, CaC_{12}−$7H_2$, and Ca_3C_{12}−$21H_2$ systems to study thermal stability. Our results confirm the potential of Ca-decorated carbyne for hydrogen storage.

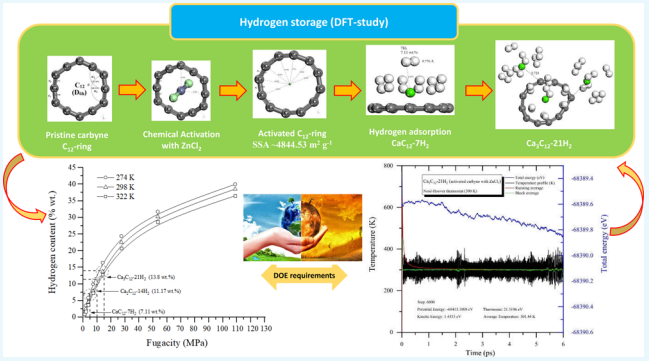

INTRODUCTION

The aim here is to determine hydrogen storage properties on a carbyne C_{12}-ring structure through chemical activation with zinc dichloride ($ZnCl_2$) and decorated with calcium atoms, by density function theory (DFT) calculations. In order to know the increasing demands necessary to hold common living standards while at the same time avoiding resource reduction and environmental pollution, there is a necessity for the growth of high-efficiency, low-cost, and eco-friendly energy storage systems.[1] As we all know, hydrogen is an ideal clean energy source that could one day replace fossil fuels, particularly for transportation applications, and combat global warming. One of the principal challenges in the growth of this technology is a compact, safe, and accessible storage system. A desirable system has to be capable of storing hydrogen with upper gravimetric density (HGD) under ambient conditions.[2−4] The U.S. Department of Energy (DOE) establishes a goal for ideal hydrogen storage materials: they ought to reach 4.5−5.5 wt % gravimetric density by the 2025 year.[5] In general, most of the studies have been dedicated to pristine carbon-based nanomaterials, such as activated carbons,[6,7] fullerenes,[8−10] graphene,[8,11] and nanotubes,[12,13] because most candidates for H_2 storage are explored owing to their low density, high thermal and chemical stability, and plainness of production; nevertheless, it has been stablished that the hydrogen storage capacity in these systems considerably diminishes at room temperature and ambient pressure,[14] being attributed to weak interactions between hydrogen molecules and carbon-based materials, due to physical adsorption (∼0.05 eV).[15] Metal doping is one of the effective methods to upgrade the strength of binding between hydrogen molecules and carbon-based nanomaterials. Alkaline-earth metal dopants, especially Ca atoms, show better hydrogen storage performance.[4,16−24] Ca atom is selected as the main dopant because of not only its lower cohesive energy (1.84 eV) compared with the transition metals (∼4 eV) but also its lightness in weight, its lower trend to aggregate on the host material whenever they are deposited, and its ability to retain the hydrogen content after doping.[20−22] Carbyne is composed of sp-

Received: November 2, 2021
Accepted: March 2, 2022
Published: March 16, 2022

https://doi.org/10.1021/acsomega.1c06149
ACS Omega 2022, 7, 10100−10114

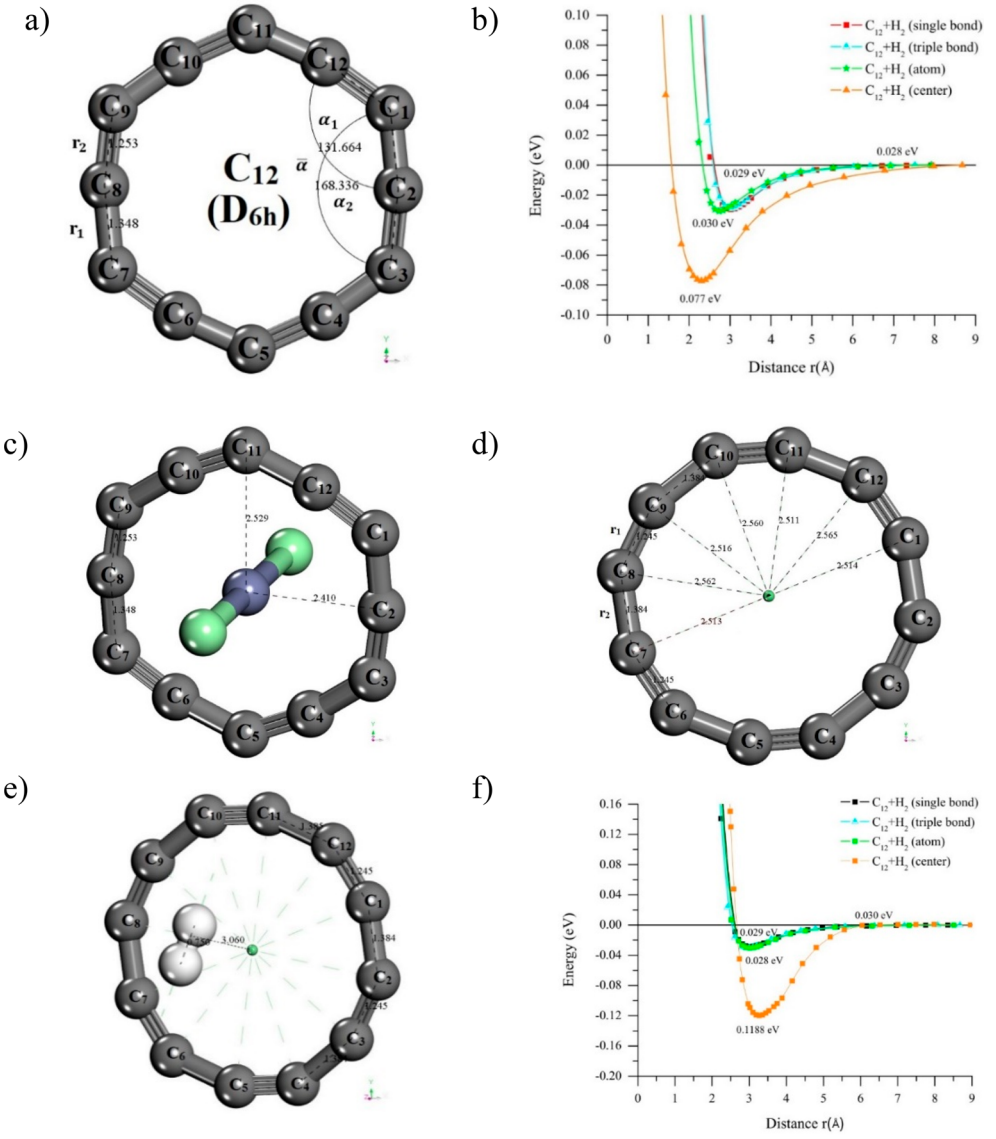

Figure 1. (a) Geometry optimization of pristine carbyne C_{12}-ring (alternating bond angles ($\bar{\alpha} = (\alpha_1 + \alpha_2)/2$) and alternating bond lengths (triple, 1.24 Å; single, 1.34 Å). (b) Bond strengths of $C_{12} + H_2$, where the H_2 molecule is adsorbed at the outer surface (single/triple bonds and in front of carbon atom) and at the inner surface (center of the ring). (c) Geometry optimization of $C_{12} + ZnCl_2$ at the center of the molecule at 2.529 and 2.41 Å (input). (d) Activated C_{12}-ring (output). (e) H_2 adsorption at the inner surface of the carbyne molecule at 3.06 Å. (f) Bond strengths of activated C_{12}-ring + H_2, where the H_2 molecule is adsorbed at the outer and the inner surfaces.

hybridized carbon atoms.[25−28] The material has been proposed as nanoelectronic and also is likely to be used for hydrogen storage owing to an effective surface area around 13,000 $m^2\ g^{-1}$, four times larger than theoretical graphene values.[18,25] The carbyne-ring structure is the base state of small carbon clusters (up to about 20 atoms) and an alternative form of linear chains, which are obtained by laser vaporization of graphite.[29−31] Between carbon clusters that result beginning with this technique in which carbyne has been found, ring structures are comparatively the most stable compared to other configurations and are the principal precursors of fullerenes and nanotubes.[32] Two carbyne structures might be defined as cumulene (equal double bonds) and polyyne (alternative single/triple bonds).[25−32] Previous research has shown theoretical estimation of Ca-decorated pristine carbyne for hydrogen storage on linear chains[18] and rings,[21] which meet the U.S. Department of Energy target requirement of 5.5 wt %.[5] Nevertheless, a single calcium atom can bind with binding energy higher than the cohesive energy, which makes cluster formation energetically favorable in these systems. To increase hydrogen storage properties on pristine carbyne molecule and enhance the binding energy of subsequent Ca atoms on carbyne, the carbyne ring has been activated through chemical activation with $ZnCl_2$ to upgrade the superficial area, and enhance pore size distribution (PSD).

Chemical activation with KOH, NaOH, H_3PO_4, or $ZnCl_2$ is a process where an activating agent is aggregated into the carbon precursor prior to pyrolysis at a temperature normally in the 450−900 °C range.[1,8,33,34] The chemical agents help to develop porosity by means of dehydration ($ZnCl_2$ or H_3PO_4) and degradation of the biomass structure, especially when the activation agent is highly alkaline (KOH).[1,33] Among the various activation agents, $ZnCl_2$ activation reacts with lignocellulosic precursor at T < 500 °C, producing a template effect and inducing a uniform micropore formation. The surface areas are normally between 1500 and 2000 $m^2\ g^{-1}$ with pore volumes <

https://doi.org/10.1021/acsomega.1c06149
ACS Omega 2022, 7, 10100−10114

1.5 $cm^3\ g^{-1}$, and the broad pore size distribution increases with the concentration of $ZnCl_2$.[1,33,35] The highest hydrogen adsorptions at 77 K and 1 bar reported for any natural and synthetic activated carbon material derived are 3.28 wt % from hemp stem,[36] 2.85 wt % from petroleum pitch,[37] and 2.96 wt % from NAC-1.5-600[34,38] when the activating agent is KOH. For $ZnCl_2$, the storage capacities obtained on CH_4 and CO_2 are 13 $cm^3\ g^{-1}$ from oil palm shell[39] and 1.3 mmol g^{-1} from rice husk,[40] respectively. Overall, the specific surface area (SSA) is key to not just enhancing H_2 storage but also achieving a higher electrochemical capacitance in terms of power delivery rate and energy storage.[41] So, in this study, we have investigated how functionalization with Ca atoms on activated carbyne with $ZnCl_2$ could influence the hydrogen storage ability. The results show adsorption energy which corresponds to chemisorption between activated carbyne and dopant agents and agreed with gas adsorption on a solid surface; with clarity we found physical adsorption between Ca atoms and hydrogen molecules. In addition, we have studied hydrogen desorption temperatures with respect to the equilibrium pressure by using the van't Hoff equation, and we determine the equilibrium pressure for the Ca-decorated carbyne by means of adsorption isotherms, to thoroughly evaluate the potential of carbyne as a hydrogen storage material.

RESULTS

To carry out the analysis of this work, we take the pristine C_{12}-ring[21] previously investigated and then we activate with zinc dichloride ($ZnCl_2$) in order to grow the surface area and enhance pore size distribution, with the aim of improving its hydrogen storage properties. The C_{12}-ring corresponds to a C_{4N} structure with $N = 3$; with a $D_{(n/2)h}$ symmetry.[31,32] Figure 1a shows geometry optimization of pristine carbyne C_{12}-ring with alternating single/triple bonds, called polyyne, where the most general case is linear acetylene (H−C≡C−H).[25,27,42] First, to estimate the H_2 adsorption capacity on the pristine carbyne without calcium attachment, we use two measures: specific surface area (SSA)[43] and accessible surface area (ASA).[44] The SSA method is based on the geometrical calculation of the area, whereas the ASA method is based on the Monte Carlo integration technique where the probe molecule is "rolled" over the framework surface. The SSA calculations of pristine and activated carbyne C_{12}-ring have been carried out by inserting triangles on the ring using the Heron formula, eq 1.[45]

$$A = \sqrt{P(P-a)(P-b)(P-c)} \tag{1}$$

where P is the perimeter of a triangle with a, b, and c sides, whereas the PSD is calculated as an approximation to the circle area.

Using eq 1, we calculated the area and pore diameter showing values of 18.37 $Å^2$ and 4.83 Å, respectively. With these results, we calculated the SSA[43] of pristine carbyne, showing a value of 4606.31 $m^2\ g^{-1}$, whereas ASA[44] shows a value of 13000 $m^2\ g^{-1}$, according to Biovia Materials Studio Software and the Monte Carlo integration technique. Second, the average hydrogen binding energy on pristine and activated carbyne was calculated from the following, eq 2.[46]

$$E_b = (E_{C_{12}-nH_2} - E_{C_{12}} - N_H E_H)/N_H \tag{2}$$

where N_H is the number of hydrogen atoms physisorbed on the inner and outer surfaces of pristine and activated carbyne C_{12}-ring, $E_{C_{12}-nH_2}$ and $E_{C_{12}}$ are the total energies of the hydrogenated carbyne ring and corresponding pristine and activated C_{12}-ring, respectively, and E_H is the energy of an isolated hydrogen atom. As in the cases of graphene,[8] CNTs,[12] and C_{60},[13] hydrogen adsorption on pristine C_{12}-ring is due to weak van der Waals (vdW) interactions. The adsorption energy of a single H_2 molecule to the outer and inner surfaces of pristine carbyne only reaches adsorption energies of 0.077 and 0.028 eV, respectively. The next hydrogen molecules added to the host material on the inner and outer surfaces diminish the binding energy until 0.01 eV; this means that the pristine carbyne is not a good candidate for hydrogen storage directly. The interactions are evident through the potential energy surfaces (PESs), which give the minimum $E(r)$ and correlate with the equilibrium point later to geometry optimization of the interacting system (C_{12} + H_2) on the outer and inner surface of pristine carbyne. Figure 1b shows the bond strengths of C_{12} + H_2, where the H_2 molecule is adsorbed at the outer and at the inner surfaces. The resulting values show the dissociation energy to form C_{12} + H_2 corresponding to physisorption,[47] which involves binding hydrogen molecules to the host material and requires very low temperatures and high hydrogen gas pressure.

Subsequently, through chemical activation with zinc dichloride ($ZnCl_2$), we activate the pristine carbyne to increase the surface area and enhance PSD. In widespread terms, these characteristics are central to not only enhancing hydrogen storage but also achieving the best work in power distribution rate and energy storage. We place a $ZnCl_2$ molecule to the center of the pristine C_{12}-ring at 2.529 and 2.410 Å distances as shown in Figure 1c. By applying geometry optimization and removing $ZnCl_2$, the area and pore size diameter result in 19.32 $Å^2$ and 4.96 Å, respectively, using eq 1, representing increases of 5.17% and 2.69% with respect to pristine C_{12}-ring (Figure 1d). In addition, we calculate the SSA and ASA of activated carbyne C_{12}-ring as a function of their geometrical characteristics. The obtained values show ∼4844.53 $m^2\ g^{-1}$ (SSA) and 15047.88 $m^2\ g^{-1}$ (ASA), which represents a macroscopic parameter that might be the kind to modify the synthesis condition of carbyne molecules. Even more, from literature, activated carbon shows a surface area of fewer than 2000 $m^2\ g^{-1}$[37] and cannot be used for hydrogen storage. Activated carbyne ring represents an alternative due to high specific surface area as a hydrogen storage material. Then, we investigate the hydrogen adsorption of a single H_2 molecule as much at the outer as the inner surface of activated C_{12}-ring (Figure 1e). The results show that only in the center of the C_{12}-ring the H_2 molecules might be adsorbed; however, only two H_2 molecules may be adsorbed with an adsorption energy higher than ∼0.1 eV. The outer zones of the activated C_{12}-ring only reach an adsorption energy of ∼0.030 eV (Figure 1f), which corresponds to lower adsorption energies for hydrogen storage at environmental conditions. These results are compared against toroidal carbon nanostructure C_{120},[46] where hydrogen adsorption energies are lower by 0.1 eV per H_2; a full hydrogen storage uptake of 2.05 wt % is for 15 H_2 molecules adsorbed at the inner surface of the toroidal carbon C_{120}. The same case is observed for the activated C_{12}-ring, where the full hydrogen storage capacity is 2.72 wt % with only two H_2 molecules adsorbed at the inner surface, which do not meet the goals established by the DOE. Although there is an upgrade in hydrogen adsorption on activated carbyne, this makes it impractical for mobile applications, just like a pristine carbyne ring. However, this is a good start for future research to address this.

https://doi.org/10.1021/acsomega.1c06149
ACS Omega 2022, 7, 10100−10114

Table 1. Average Energy, Adsorption Energy of the *n*th H_2 Molecule on the Doped Complex (eV) and Binding Energy of CaC_{12} (eV)

				$CaC_{12}-nH_2$ (eV)						
position	functional	energy (eV)	E_b^{Ca} (eV)	$1H_2$	$2H_2$	$3H_2$	$4H_2$	$5H_2$	$6H_2$	$7H_2$
triple	DFT-D	E_{av}	2.79	0.5362	0.4346	0.4143	0.4132	0.4103	0.4018	0.3938
		E_{ad}		0.5362	0.3331	0.3735	0.4101	0.3987	0.3591	0.3457
single	DFT-D	E_{av}	2.79	0.4515	0.4278	0.4124	0.4062	0.4019	0.4034	0.3983
		E_{ad}		0.4515	0.4041	0.3817	0.3876	0.3848	0.3907	0.3681
center	DFT-D	E_{av}	3.34	0.3818	0.3454	0.3502	0.3176	0.3293	0.3929	0.3706
		E_{ad}		0.3818	0.3091	0.3398	0.3011	0.3161	0.3105	0.3015
wt %				1.0825	2.1418	3.1787	4.1938	5.1879	6.1615	7.1154

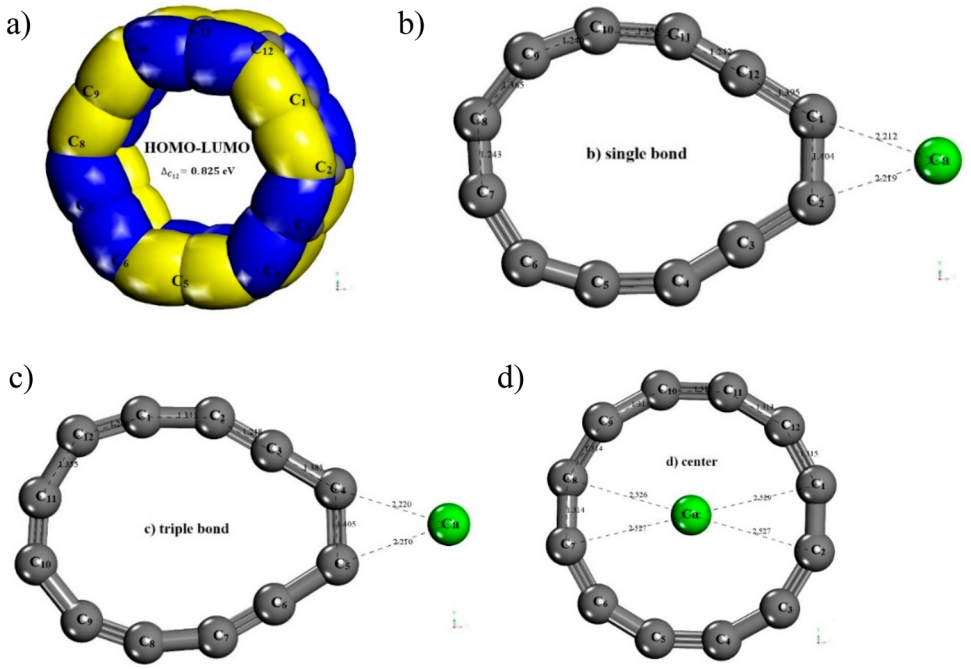

Figure 2. (a) HOMO−LUMO spatial distribution of activated carbyne C_{12}-ring with $ZnCl_2$. Blue lobes display positive values and yellow lobes negative values of the wave function, with an energy difference of $\Delta_{C_{12}} = 0.825$ eV. Optimal position of Ca atom on activated C_{12}-ring (b) in front of the single bond (C_1-C_2), (c) in front of the triple bond ($C_4\equiv C_5$), and (d) within the ring.

Subsequently, we studied the behavior of Ca-doped activated carbyne with $ZnCl_2$. The modeling of the Ca−carbyne complex considers several starting configurations at the inner and outer surfaces (in front of single and triple bonds and at the center of the activated carbyne ring) separated at 2.48 Å, and we examine the Ca−carbyne stability by determining the binding energy (E_b^{Ca}) using eq 3.[19,20,48]

$$E_b^{Ca} = \frac{1}{x}[E_{C_{12}} + xE_{Ca} - E_{Ca_xC_{12}}] \quad (3)$$

where $E_{C_{12}}$ is the total energy of the activated carbyne molecule, E_{Ca} is the total energy per calcium atom, and $E_{Ca_xC_{12}}$ is the total energy of one carbyne molecule with x Ca atoms. For a single Ca atom, we find three optimal positions around the C_{12}-ring to be located in front of either single or triple bonds and also at the center of the ring, with binding energies of 2.79 eV (single and triple bonds) and 3.34 eV (center of the ring), which with respect to the pristine CaC_{12} complex[21] represent increases of 25.11% and 49.77%, respectively, which means it is strongly chemisorbed.[47] (Table 1).

As a note, unlike the pristine CaC_{12} complex, only the single bond C_1-C_2, C_5-C_6, or C_9-C_{10} was the better zone for calcium atoms; these zones present the blue lobes for HOMO−LUMO spatial distribution. For activated C_{12}-ring we found a better HOMO−LUMO distribution (Figure 2a) around the ring, where the Ca atom prefers to bind indistinctly in any zone of carbyne C_{12}-ring. Here, the positive value of E_b^{Ca} means that the doped complex is thermodynamically stable. In addition, our results of binding energy values were higher than those of fullerenes,[16] carbon nanotubes,[17] carbyne chains,[18,21] graphene,[23] and heterofullerenes.[20] Therefore, this indicates that cluster formation is energetically unfavorable, so this factor will not diminish the possible hydrogen capacity on activated C_{12}-ring. Panels b−d of Figure 2 show the geometry optimization of the activated doped complex. The calcium atom tends to extend the double and single bonds to the activated carbyne to 1.404 and 1.405 Å, respectively, and how the Ca atom is adsorbed at the center of the ring.

In addition, we have also achieved DFT-based molecular dynamics (MD) simulations for both C_{12} and CaC_{12} systems in their forms pristine and activated with $ZnCl_2$. All of the

https://doi.org/10.1021/acsomega.1c06149
ACS Omega 2022, 7, 10100−10114

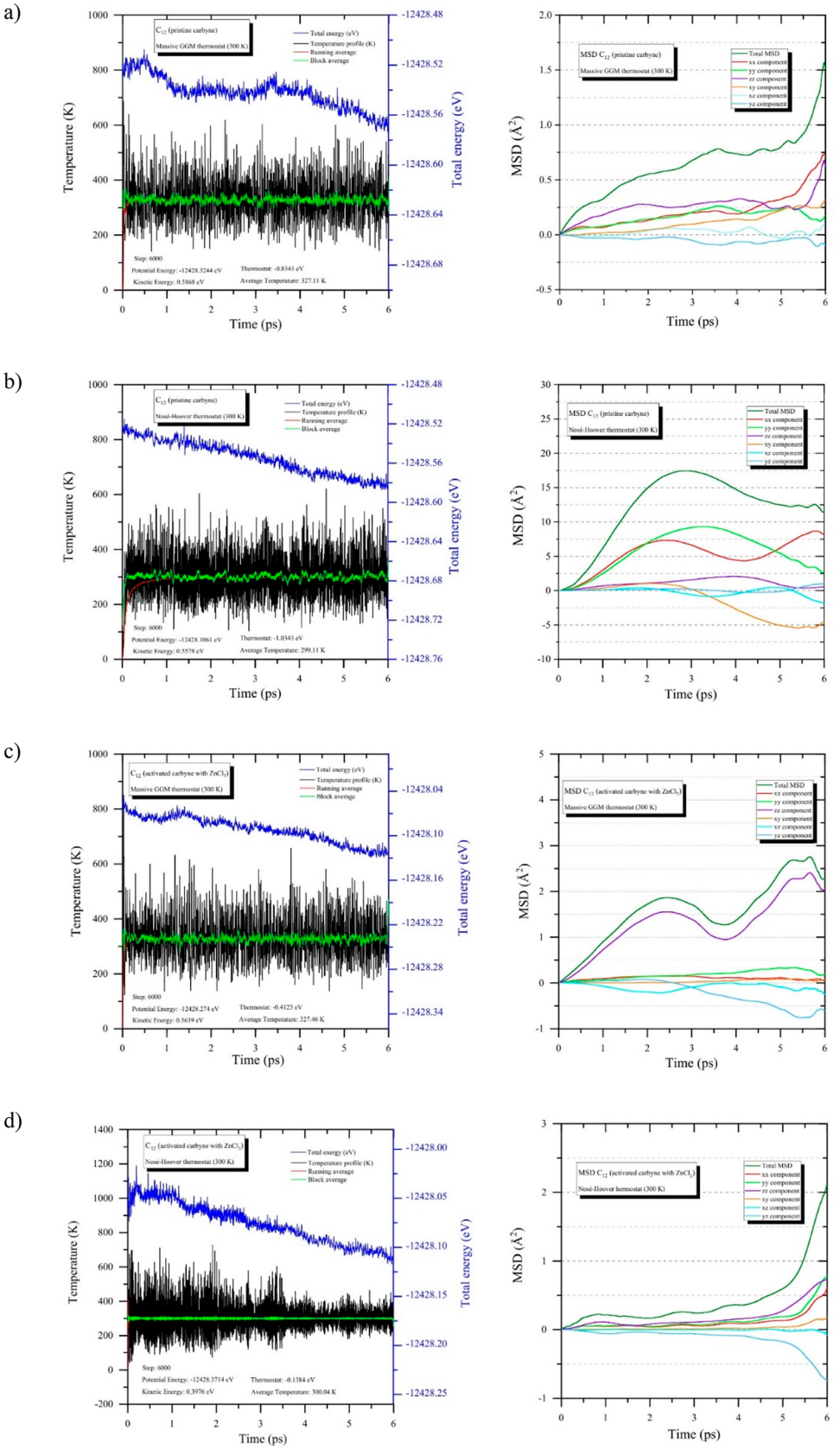

Figure 3. continued

https://doi.org/10.1021/acsomega.1c06149
ACS Omega 2022, 7, 10100−10114

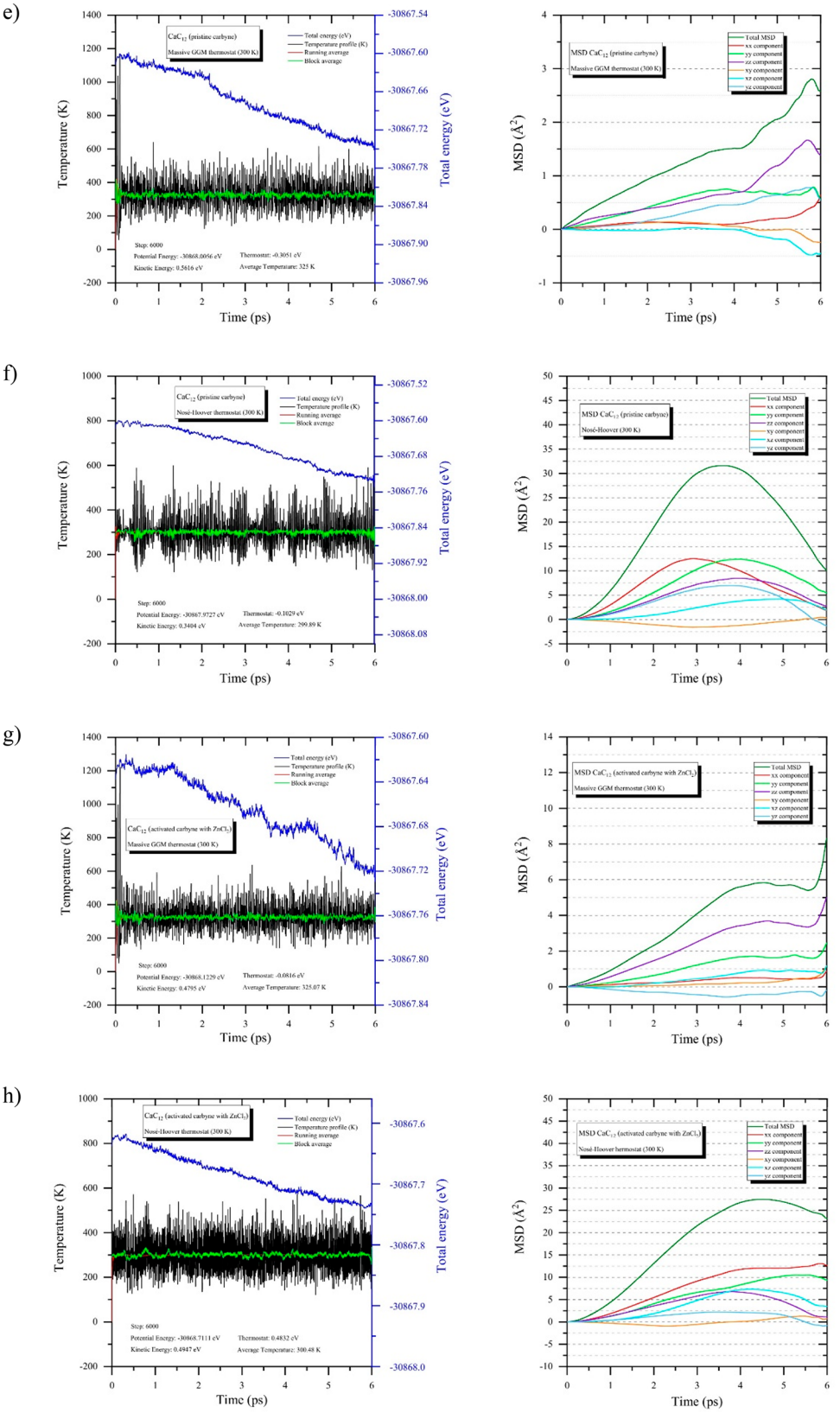

Figure 3. Molecular dynamics (MD) production run of the C_{12}-ring and calcium-decorated carbyne after 6 ps with massive GGM and Nosé−Hoover thermostat. (a, b) Pristine carbyne C_{12}-ring. (c, d) Activated carbyne C_{12}-ring with $ZnCl_2$. (e, f) Calcium-deocrated carbyne CaC_{12} (pristine). (g, h) Calcium-decorated carbyne CaC_{12} (activated with $ZnCl_2$).

simulations were achieved in an *NVT* ensemble (constant number of atoms, volume, and temperature) with a specific temperature of 300 K. The molecular dynamic simulations were run for 6 ps, with 1 fs as a time of step, using massive GGM[49] and Nosé−Hoover[50−52] thermostat to address the structural and thermal stabilities of the system (Figure 3a−h). Our results after

https://doi.org/10.1021/acsomega.1c06149
ACS Omega 2022, 7, 10100−10114

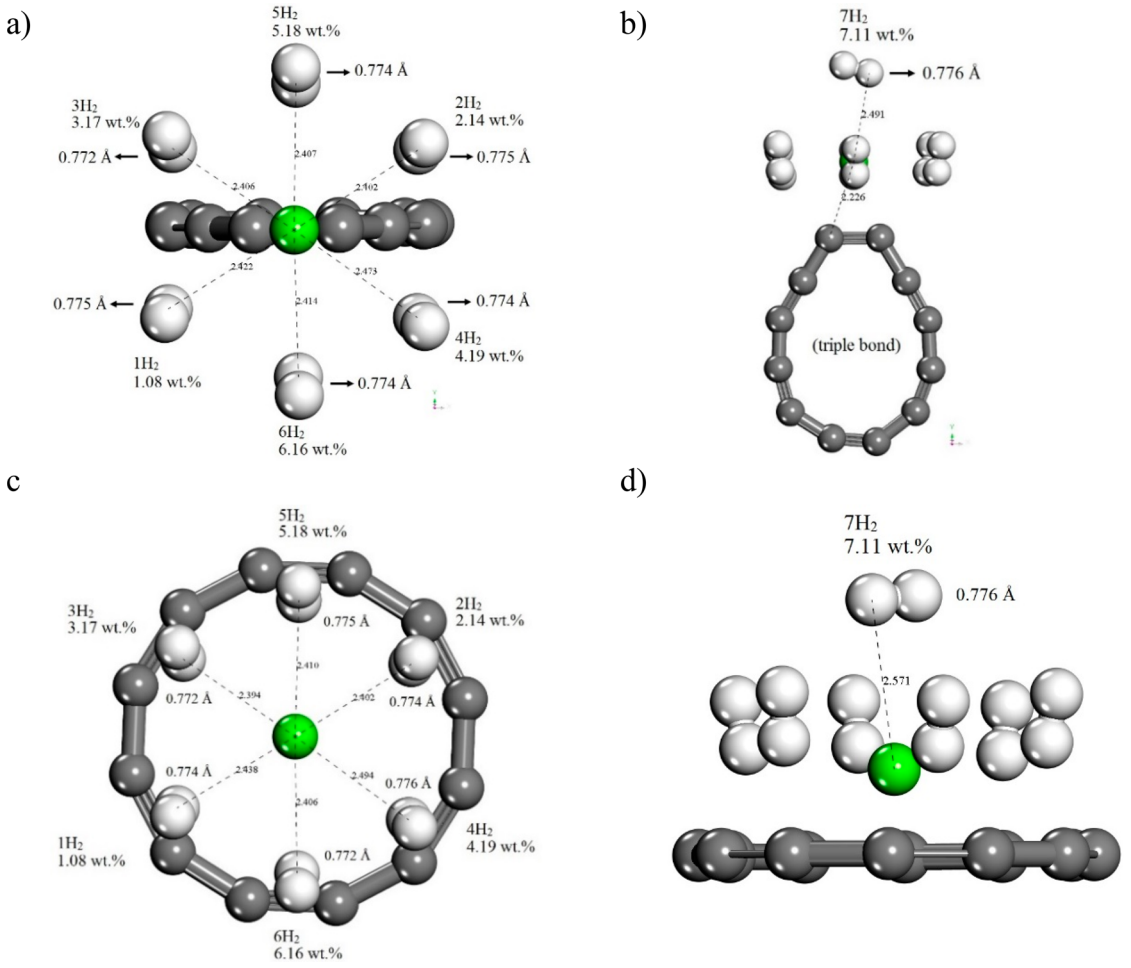

Figure 4. Geometry optimization scheme for activated CaC_{12}–nH_2, with n = 1–7 H_2 molecules adsorbed onto the doped complex. (a–d) Hydrogen adsorption on DFT-GGA-PBE with the empirical correction scheme of Grimme (DFT-D), where the first six H_2 molecules are adsorbed around the Ca atom and the seventh H_2 molecule is on top of the Ca atom. The configuration of H_2 molecules in the doped complex is observed as gray color for carbon atoms, white color comprises H_2 molecules, and green color corresponds to the decoration Ca atoms.

6 ps of MD production show better thermal stabilities of all activated structures with Nosé–Hoover thermostat at 300 K. Every system was equilibrated for 3–6 ps, and after 5 ps of production, no breaking of bonds was observed, which implied the thermal stability of C_{12} and CaC_{12} systems. The average temperature of the MD production run for pristine carbyne C_{12}-ring is 327.11 K and 299.11 K for massive GGM and Nosé–Hoover thermostat, respectively, along the 6 ps MD production run. For activated C_{12}-ring the average temperature was 327.46 K and 300.04 K for massive GGM and Nosé–Hoover thermostat, respectively. The mean square displacement (MSD) is shown in Figure 3a–h for all of the systems (C_{12}-ring and Ca-decorated carbyne). To summarize, the run of MD production showed that activated CaC_{12} is a good candidate since this structure after 6 ps retains its initial properties without too much variation in bond lengths and considerably lower temperatures, which implied good thermal stability of activated carbyne. In addition, using the Nosé–Hoover thermostat we have carried out an MD production run at 200 and 100 K for the carbyne C_{12}-ring and doped complex CaC_{12} (pure and activated) that is shown in the Supporting Information.

Through Mulliken population analysis and electrostatic potential (ESP)-fitted charges, we observe positive charge on the Ca atom toward the carbyne ring, which results in (+0.949e and +1.056e), (+0.944e and +1.052e), and (+0.99e and +1.464e) for a single bond, triple bond, and center of carbyne molecule, respectively. As shown in the Supporting Information, we added the charge-transfer mechanism of carbyne C_{12}-ring and doped complex CaC_{12}–nH_2 with n = 1–7 H_2 molecules adsorbed around the Ca atom for pristine and activated carbyne with $ZnCl_2$.

Once the CaC_{12} activated complex reaches equilibrium, the next step is the adsorption analysis of H_2 molecules on the decorated complex. Using eqs 4 and 5,[4,18,20,21] we calculate the average binding energy and adsorption energy of nH_2 molecules adsorbed on the doped complex.

$$E_{av} = \frac{[E_{(Ca_xC_{12})} + nE_{(H_2)} - E_{(Ca_xC_{12}-nH_2)}]}{n} \quad (4)$$

$$E_{ad} = E_{(Ca_xC_{12}+(n-1)H_2)} + E_{(H_2)} - E_{(Ca_xC_{12}-nH_2)} \quad (5)$$

where $E_{(Ca_xC_{12})}$ and $E(_{H_2})$ are the total energies of the Ca_xC_{12} complex and an isolated H_2 molecule, respectively. The $E_{(Ca_xC_{12}-nH_2)}$ is the total energy of the Ca_xC_{12} system with nH_2 molecules and $E_{(Ca_xC_{12}+(n-1)H_2)}$ is the total energy of the Ca_xC_{12} system with $(n-1)$ H_2 molecules adsorbed on the doped complex. The next H_2 molecules were placed one by one around the Ca atom until there were seven H_2 molecules. The average energy and adsorption energy results of the nth H_2 molecule

https://doi.org/10.1021/acsomega.1c06149
ACS Omega 2022, 7, 10100–10114

Table 2. Hydrogen Storage on Carbon-Based Materials Theoretical (DFT) and Experimental Calculations

system	type of study	react agent/dopants	storage condition	storage capacity	ref
activated-CNF-KOH	experimental	KOH	303 K/10 MPa	0.42 wt %	6
activated-NF-KOH				0.1 wt %	7
activated-MWCNT-KOH	experimental	KOH	298 K/20 MPa	0.2 wt %	
KUA1				0.5 wt %	
KUA5				3.2 wt %	
natural material-derived activated carbon from hemp stem with KOH	experimental	KOH	77 K and 1 bar	3.28 wt %	36
synthetic material-derived activated carbon from petroleum pitch with KOH	experimental	KOH	77 K and 1 bar	2.85 wt %	37
synthetic material NAC-1.5−600 (KOH)	experimental	KOH	77 K and 1 bar	2.96 wt %	34, 38
oil palm shell	experimental	$ZnCl_2$	CA for methane adsorption (CH_4)	13 cm^3/g	39
rice husk	experimental	$ZnCl_2$	CA for carbon dioxide adsorption (CO_2)	1.3 mmol/g	40
lignin	experimental	H_2SO_4	CA for H_2 adsorption	1.89 wt %	53
palm stone	experimental	H_3PO_4	CA for carbon dioxide adsorption (CO_2)	2.7 mmol/g	54
graphene	experimental	Pd	ambient conditions/50 MPa	6.7 wt %	55
B_{28}	theoretical (DFT)	Na	desorption temperature of 300 K/0.1 MPa	7.99 wt %	2
		Ca		6.67 wt %	
		K		6.30 wt %	
		Mg		6.05 wt %	
		Y		5.99 wt %	
		Li		6.96 wt %	
B-graphene	theoretical (DFT)	Ca	∼0.4 eV H_2^{-1}	8.38 wt %	3
graphyne	theoretical (DFT)	Ca	$4H_2$ adsorbed at 298 K/3 MPa	9.6 wt %	4
fullerene C_{60}	theoretical (DFT)	Ca	$5H_2$ adsorbed (∼0.2 eV per H_2); binding energy of CaC_{60}, 1.3 eV, causing clustering	8.4 wt %	16
carbyne	theoretical (DFT)	Ca	$4H_2$ are adsorbed at 300 K/5 MPa	8 wt %	18
heterofullerene ($C_{48}B_{12}$)	theoretical (DFT)	Ca	$5H_2$ adsorbed at $T \leq 150$ K $6H_2$ desorbed at $T \geq 300$ K	7.1 wt %	20
Carbyne C_{12}-ring	Theoretical (DFT)	Ca	$6H_2$ adsorbed with average energy of 0.32 eV H_2^{-1}	6.16 wt %	21
Carbyne C_{10}-ring	Theoretical (DFT)	Ca	$7H_2$ adsorbed with average energy of 0.26 eV H_2^{-1}; equilibrium pressure, 18−37 MPa	8.09 wt %	24
carbyne	theoretical (DFT)	Li	$3H_2$ are adsorbed per Li atom with adsorption energy (200−600 meV)	7.1 wt %	14
α-B sheet	theoretical (DFT)	Ca	300 K/10 MPa	8.72 wt %	22
Zeolite templated carbon (ZTC)	Theoretical (DFT)	Li	298 K/35−50 MPa	6.78 wt %	48, 56

adsorbed by CaC_{12} complex using eqs 4 and 5 are summarized in Table 1. In Figure 4, we legibly illustrated the process of attaching molecules to the CaC_{12}, performed by setting one by one until a maximum of seven H_2 molecules.

We determine that the first six H_2 molecules tend to be adsorbed around the calcium atom, and the seventh H_2 molecule is physically adsorbed on the upper side of the calcium atom. The optimized systems of $CaC_{12}-7H_2$ are rather similar for single and triple bonds; therefore, we only take the triple bonds and center to properly put each one of the seven H_2 molecules adsorbed on the doped complex. The first H_2 molecule is adsorbed on the doped complex with an average energy and adsorption energies of 0.5362, 0.4515, and 0.3818 eV per H_2, when the Ca atom is placed in front of single and triple bonds and the center of the activated carbyne molecule, respectively (see Table 1). To determine the relationship between the Ca−H_2 distance and the H_2 adsorption energy, according to the literature[19] if the Ca−H_2 distances are less than 3 Å the adsorption energies are greater than 0.2 eV per H_2.

Therefore, in our case, we observed that each of the Ca−H_2 distances is in the range of 2.3−2.6 Å, and the H−H average bond length is 0.774 Å for all orientations. The next added molecules to the CaC_{12} are maintained with an average energy E_{av} = (0.4145, 0.4291, and 0.3554 eV) per H_2 and adsorption energy E_{ad} = (0.3983, 0.3937, and 0.3369 eV) for single and triple bonds and the center of the carbyne molecule, respectively. Therefore, in this study with correction of Grimme calculations, we determine that the CaC_{12} complex might adsorb until seven H_2 molecules per Ca atom with enough energy and quantity of hydrogen for using it as a storage material. The weight percent (wt %) of H_2 molecules in a carbyne Ca_xC_{12} are also calculated with eq 6.

$$\text{wt \%}H_2 = \left[\frac{m_{H_{2ads}}}{m_{H_{2ads}} + m_{CaC_{12}}}\right] \times 100 \quad (6)$$

where $m_{H_{2ads}}$ is the mass of H_2 molecules adsorbed on the decorated complex, and the mass of Ca_xC_{12} decorated complex is $m_{CaC_{12}}$. The hydrogen storage capacity obtained in this study is 7.11 wt % (Table 1). Thus, the maximum hydrogen storage capacity is greater than the capacity ∼6 wt % of the Ca-decorated carbyne (polyyne),[18,21] 7 wt % Ca-decorated boron heterofullerenes,[20] ∼5 wt % Ca-decorated carbon nanotubes,[17] by theoretical DFT calculations, and other activated carbons by using several activating agents such as KOH, $ZnCl_2$, H_2SO_4, and H_3PO_4 (see Table 2).

https://doi.org/10.1021/acsomega.1c06149
ACS Omega 2022, 7, 10100−10114

Subsequently, we saturate the doped complex by placing up to three Ca atoms on the mentioned positions (single and triple bonds and the center of the ring) and we observe binding energies above 2.8 eV for the second and third Ca atoms, which show stability in the system, indicating that the cluster formation is energetically unfavorable as an increase the calcium atoms concentration in the system. We repeat the same methodology of adding H_2 molecules to the Ca atoms, even to which $7H_2$ molecules per Ca atom might bind, with an average binding energy of ~0.36 eV per H_2, obtaining a Ca_3C_{12}−$21H_2$ system. This study reaches 13.8 wt % for the gravimetric density, fulfilling DOE requirements. However, this gravimetric density requires experimental investigation to be validated and makes it very feasible that the system can only absorb up to one Ca atom.

As the next step, we built potential energy surfaces for doped complex CaC_{12}−nH_2 with n = 1−7 hydrogen molecules adsorbed on it. The methodology to accomplish potential energy curves for the hydrogen molecules adsorbed by Ca atom is to perform a geometry optimization for each H_2 molecule added to the doped complex as a first step, which provides the minimum energy and distance corresponding to the equilibrium point of each system. Then, single-point calculations by oscillating ±4 Å around the minimum energy with steps of 0.02 Å to calculate energies at each point and build potential energy surfaces, $E(r)$. Figure 5 shows PES for the seven H_2 molecules adsorbed on activated doped complex when the Ca atom is placed in front of a single bond of carbyne molecule. All of the minimum energies obtained and calculated by eq 4 are equivalents and provide information about the $7H_2$ molecules that were physically adsorbed by calcium atoms (see Table 1 and Figure 5).

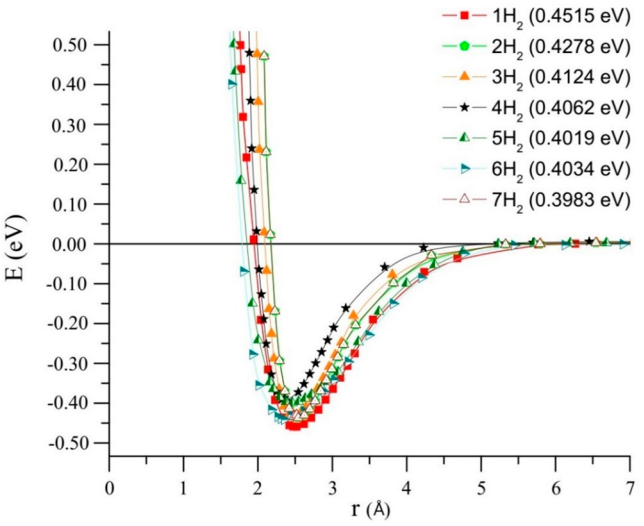

Figure 5. Potential energy surfaces (PESs) corresponding to the CaC_{12}−$7H_2$ system.

We carry out HOMO−LUMO calculations for the CaC_{12}−$7H_2$, which is observed in Table 3. We clearly observed that values of energy difference for the doped complex are about 0.926−0.960 eV for the single bond, 0.925−0.965 eV for the double bond, and 0.13−0.6 eV for the center of the carbyne molecule, indicating that the doped complex is stable enough.

We determine the isothermal curves at three temperatures (274, 298, and 322 K) for the CaC_{12}−$7H_2$ and Ca_3C_{12}−$21H_2$ systems using the Sorption program as described in Computational Methods. The equilibrium pressure with the fitting curve when we have 7.11 wt % for the CaC_{12}−$7H_2$ system and 13.8 wt % for the Ca_3C_{12}−$21H_2$ system, since they present energies in the desirable range of 0.2−0.6 eV, for hydrogen storage. Therefore, the equilibrium pressure lies in the range of 5−15 MPa as shown in Figure 6.

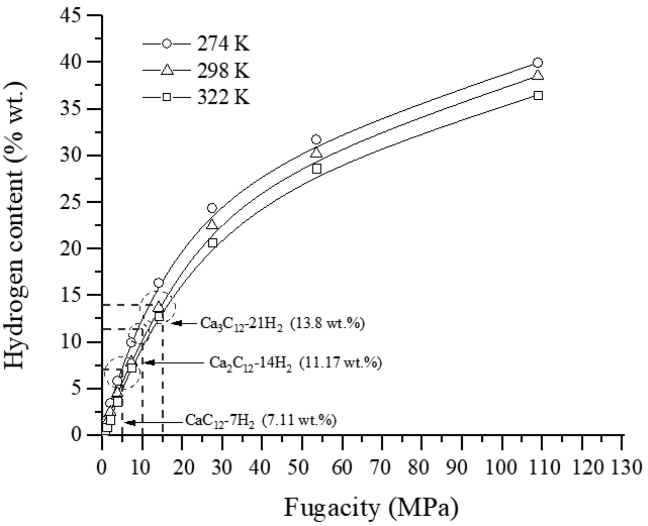

Figure 6. Isothermal curves at three temperatures (274, 298, and 322 K), when we have 7.11 and 13.8 wt %, which corresponds to CaC_{12}−$7H_2$ and Ca_3C_{12}−$21H_2$ systems. The equilibrium pressures from the fitting curve when we have 7.11 and 13.8 wt % are in the range of 5−15 MPa.

Together with the gravimetric densities, the thermal stability of adsorbed H_2 on activated complex should be investigated as it plays an indispensable role in predicting the effectiveness of hydrogen charge/discharge cycles. The thermal stability correlates with the binding energy of hydrogen to the storage

Table 3. HOMO−LUMO Energy Difference or Gap (Δ, eV) of CaC_{12} and CaC_{12}−$7H_2$

	single bond			triple bond			center		
system	HOMO (eV)	LUMO (eV)	Δ	HOMO (eV)	LUMO (eV)	Δ	HOMO (eV)	LUMO (eV)	Δ
CaC_{12}	−4.292	−3.332	0.960	−4.295	−3.33	0.965	−5.206	−4.601	0.605
CaC_{12}−H_2	−4.222	−3.290	0.932	−4.238	−3.301	0.937	−5.240	−4.782	0.458
CaC_{12}−$2H_2$	−4.137	−3.211	0.926	−4.196	−3.271	0.925	−5.240	−5.103	0.137
CaC_{12}−$3H_2$	−4.211	−3.261	0.950	−4.182	−3.233	0.949	−5.272	−5.061	0.211
CaC_{12}−$4H_2$	−4.201	−3.251	0.950	−4.215	−3.261	0.954	−5.275	−5.079	0.195
CaC_{12}−$5H_2$	−4.207	−3.273	0.934	−4.224	−3.283	0.941	−5.246	−5.050	0.196
CaC_{12}−$6H_2$	−4.233	−3.292	0.941	−4.232	−3.297	0.935	−5.181	−5.013	0.168
CaC_{12}−$7H_2$	−4.223	−3.281	0.942	−4.241	−3.301	0.940	−5.194	−5.025	0.169

https://doi.org/10.1021/acsomega.1c06149
ACS Omega 2022, 7, 10100−10114

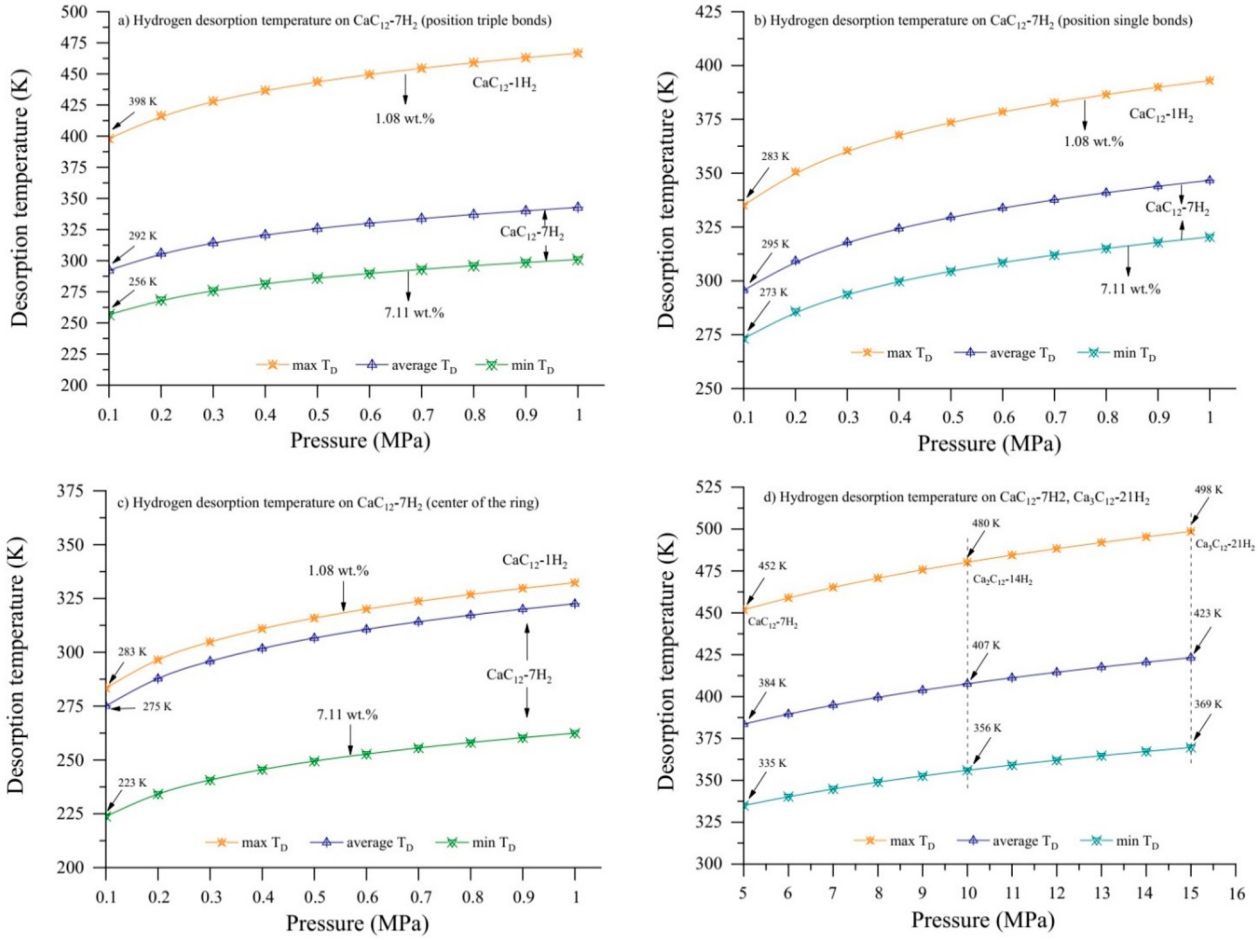

Figure 7. (a−d) Dependence of hydrogen desorption temperature on the equilibrium pressure. (a−c) Average T_D (blue line), onset T_D (of H_2 gravimetric density of 7.11 wt.%; green line), and the highest T_D (1.08 wt %; orange line), which correspond to different positions where the Ca atom can bind to activated carbyne. (d) Desorption temperature on equilibrium pressure of 5−15 MPa for CaC_{12}−$7H_2$, Ca_2C_{12}−$14H_2$, and Ca_3C_{12}−$21H_2$ doped complexes.

material.[14] Here, we are using eq 7 (van't Hoff equation) to estimate the desorption temperature.

$$T_D = E_{ad}/k_B[(\Delta S/R) - \ln p]^{-1} \quad (7)$$

where E_{ad} is the hydrogen adsorption energy, k_B is the Boltzmann constant, ΔS is the change in the hydrogen entropy from molecular gas to dissolved solid hydrogen (standard hydrogen entropy, 130 J K^{-1} mol^{-1}),[14] R is the gas constant, and p is the equilibrium pressure (in our calculations we used the range of 0.1−1 MPa with respect to the standard atmospheric pressure).

The activated carbyne complex (shown in Figure 3) is considered as the highest gravimetric density to estimate the hydrogen desorption temperatures. Panels a−c of Figure 7 show van't Hoff desorption temperatures in the range of equilibrium pressures (0.1−1 MPa) corresponding to hydrogen gravimetric densities for the chosen structure. So, all $T_D(p)$ dependencies were obtained by employing hydrogen adsorption energies (in the case of CaC_{12}−$7H_2$ activated complex) in eq 6.

Average T_D is calculated by using E_{av} (average binding energy of seventh H_2 molecule adsorbed per Ca atom). The onset desorption temperature (min T_D) is obtained to describe adsorption energy (E_{ad}) of the seventh hydrogen molecule per Ca atom, and it corresponds to the minimal temperature, which is necessary to start hydrogen release. By using the adsorption energy of the first H_2 molecule adsorbed by Ca atom on a doped complex, we calculate the highest desorption temperature, max T_D, which is necessary to fully discharge the considered system. At normal atmospheric pressure (p = 0.1 MPa), the average T_D is 292 and 295 K (Figure 7a,b) when the Ca atom is placed in front of triple and single bonds and can adsorb until seven H_2 molecules, in the case of the center of the ring the maximum desorption temperature at 0.1 MPa is 275 K (Figure 7c), which is much higher than the critical point of hydrogen (33 K) and more than triple the boiling point to liquid nitrogen (77 K). As a note, desorption temperatures could be further increased by the increase of equilibrium pressure. On the basis of this, we take the equilibrium pressure obtained with the isothermal curves in the range (5−15 MPa) for CaC_{12}−$7H_2$, Ca_2C_{12}−$14H_2$, and Ca_3C_{12}−$21H_2$ activated complexes, and we compare the thermal stability using eq 7. Here we used the average adsorption energy of all hydrogen molecules adsorbed by the doped complex, and we give an estimate of desorption temperatures (Figure 7d). At pressures of 50, 100, and 150 MPa, the average T_D is 384, 407, and 423 K for the CaC_{12}−$7H_2$, Ca_2C_{12}−$14H_2$, and Ca_3C_{12}−$21H_2$ doped complex, respectively. The highest gravimetric densities for each of the systems are 7.11 wt % (CaC_{12}−$7H_2$), 11.17 wt % (Ca_2C_{12}−$14H_2$), and 13.8 wt % (Ca_3C_{12}−$21H_2$).

https://doi.org/10.1021/acsomega.1c06149
ACS Omega 2022, 7, 10100−10114

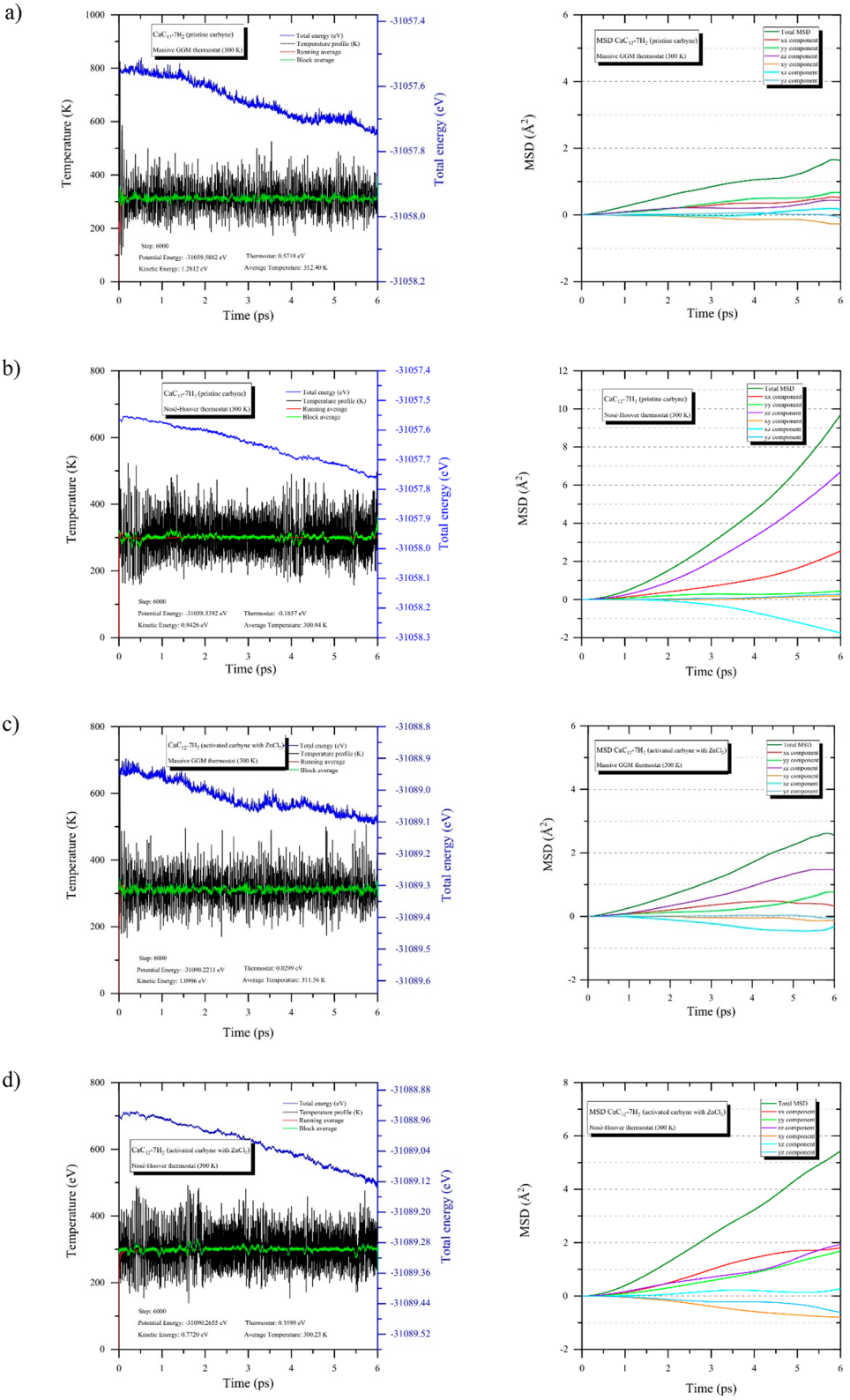

Figure 8. continued

https://doi.org/10.1021/acsomega.1c06149
ACS Omega 2022, 7, 10100−10114

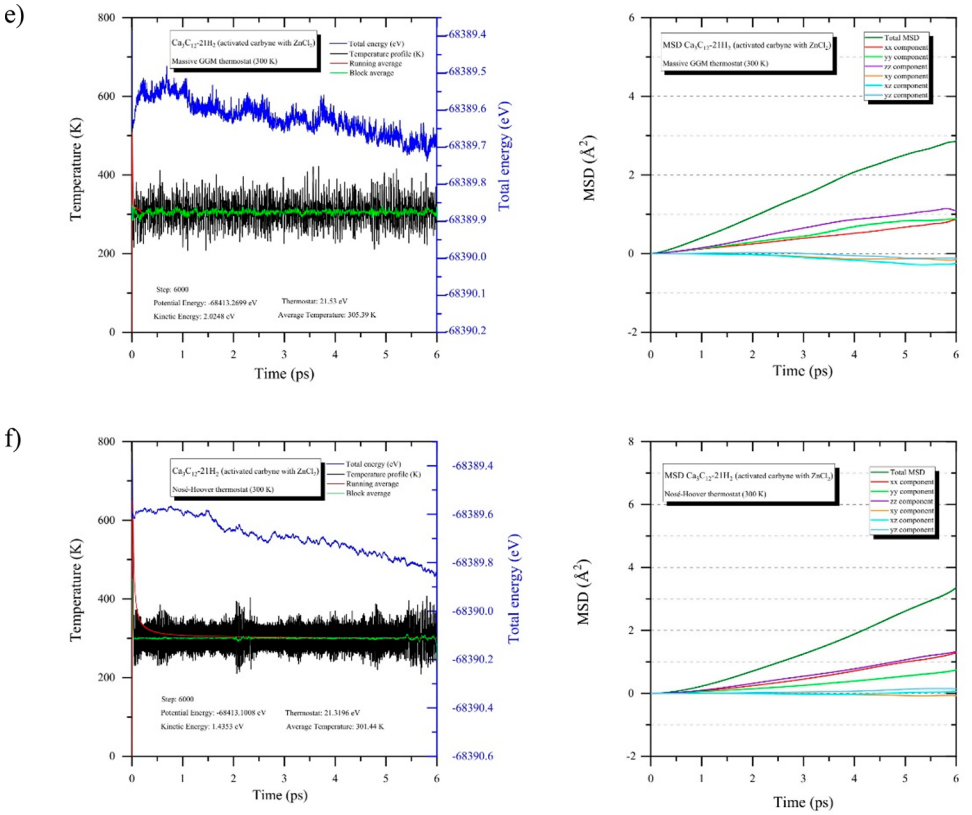

Figure 8. Molecular dynamics (MD) production after 6 ps at 300 K. (a, d) CaC_{12}−$7H_2$ (pristine and activated carbyne). (e, f) Ca_3C_{12}−$21H_2$ (activated carbyne). All MD simulations employed massive GGM and Nosé−Hoover thermostats and present the mean square displacements (MSDs).

In addition, we also performed DFT-based molecular dynamics for CaC_{12}−$7H_2$ (pristine and activated carbyne) and Ca_3C_{12}−$21H_2$ systems with massive GGM and Nosé−Hoover thermostats at 300 K. We observed unified thermal stability after 6 ps at 300 K for all molecular dynamic's simulations when the Nosé−Hoover thermostat was used. The average temperature was 300.94 K, and 300.23 K along the MD-production run for pristine and activated structures (Figure 8a−f). For doped complex Ca_3C_{12}−$21H_2$, the average temperature was 301.44 K with the Nosé−Hoover thermostat. Every system was equilibrated for 3−6 ps, and after 6 ps of production, no breaking of bonds was observed, which implied the thermal stability of the systems. In addition, using the Nosé−Hoover thermostat, we have carried out an MD production run at 200 and 100 K for the CaC_{12}−$7H_2$, and Ca_3C_{12}−$21H_2$-doped complex (pure and activated), which is shown in the Supporting Information.

Along with the previous studies in this work, we can determine that activated carbyne C_{12}-ring with zinc dichloride and decorated with Ca atoms can adsorb seven H_2 molecules with a single Ca atom with an average energy of ∼0.39 eV per H_2 molecule corresponding to 7.11 wt %. It is expected that activated C_{12}-ring might bind three Ca atoms around the inner/outer surface with their H_2 molecules, respectively, which represents an increase up to 13.8 wt % with respect to the pristine C_{12}-ring[21] previously investigated. This storage capacity satisfies the requirements established by the U.S. Department of Energy by the end of the year 2025. Therefore, the considered material might be a promising choice for efficient hydrogen storage media, so this material certainly requires further experimental investigation.

DISCUSSION

The research for hydrogen storage materials is very attractive for fuel cell applications among others. Nevertheless, it is a great challenge to find hydrogen storage materials with great hydrogen gravimetric density under ambient thermodynamic conditions. Previous studies have explored that pristine nanomaterials[6−13] cannot efficiently store hydrogen, mainly due to weak van der Waals interaction between the hydrogen molecules and host material. Pristine carbyne is not an exception; for example, in the C_{12}-ring structure only a single H_2 molecule can adsorb with adsorption energies of 0.077 and 0.028 eV at the outer and inner surfaces, respectively, by DFT calculations presented in this analysis, making unsuitable its use as a hydrogen storage material. Previous research has shown that the pristine carbyne C_{12}-ring[21] structure is the ground state. We take this structure for new experimentation, activating with $ZnCl_2$. Before chemical activation, we calculated the area of pristine carbyne and pore diameter (18.37 $Å^2$ and 4.83 Å) presented in this work. Even more, we determined the specific surface area shows a value of 4606.31 $m^2\ g^{-1}$, and accessible surface area shows a value of 13,000 $m^2\ g^{-1}$. The chemical activation helps to develop the porosity by means of dehydration with $ZnCl_2$ or H_3PO_4 of the biomass structure. In this work, we take the pure C_{12}-ring and then we activate it with $ZnCl_2$ as shown in the methodology in this work. By applying geometry optimization and removing the $ZnCl_2$, the area and pore diameter result in 19.32 $Å^2$ and 4.96 Å, respectively, representing

https://doi.org/10.1021/acsomega.1c06149
ACS Omega 2022, 7, 10100−10114

increases of 5.17% and 2.69% with respect to pristine carbyne. The SSA and ASA show values of 4844.53 $m^2\ g^{-1}$ and 15,047.88 $m^2\ g^{-1}$, respectively. These represent increases of 5.17% and 15.75% with respect to the pristine carbyne. However, the activated carbyne does not enhance the hydrogen storage properties, since only two H_2 molecules can be adsorbed with adsorption energy higher than 0.1 eV at the center of the activated carbyne, which does not meet the goals established by the DOE.

In addition, to improve the hydrogen storage properties, metal doping is one effective method to enhance the adsorption energies between H_2 molecules and host material. Previous research has shown that pristine carbyne C_{12}-ring decorated with Ca atoms might bind up to six H_2 molecules with average binding energies of 0.18 eV per H_2 (PW91) and 0.32 eV per H_2 with the empirical correction scheme of Grimme (DFT-D).[21] Nevertheless, only a single Ca atom might be bound to the carbyne molecule with binding energy (E_b^{Ca}) higher than 2 eV, reaching 6.16 wt % for the gravimetric hydrogen storage. Even for cluster C_{10}-rings[24] in polyyne and cumulenic forms, only a single Ca atom might be chemisorbed with binding energies greater than 2.5 and 2.33 eV for GGA-PW91 and GGA-PBE functionals, respectively. Up to either six or seven H_2 molecules are physisorbed by Ca atom, with average energies of 0.22 eV per H_2 (PW91) and 0.263 eV per H_2 (DFT-D) for cumulene and polyyne molecules, respectively. The hydrogen storage capacity obtained corresponds to 7.02−8.09 wt %. Thus, hydrogen storage capacities using only one Ca atom in carbyne rings reach H_2 storage capacities, which are much higher than other carbon- and boron-based materials (see Table 2), where other investigations saturate the system with more dopant atoms until reaching the goal of DOE requirements. In this work, we demonstrate that activated carbyne can bind up to three calcium atoms around this surface, with binding energy greater than 2.7 eV per Ca atom, which represents up to an increase of 49.77% with respect to the pristine CaC_{12} complex, indicating that the system is strongly chemisorbed and up to seven H_2 molecules can be physisorbed with an average energy of 0.39 eV per H_2. Reaching 13.8 wt % for gravimetric storage capacity, fulfilling the requirements by the DOE. In addition, we also performed DFT-based molecular dynamics for the C_{12} and CaC_{12} systems in their forms pristine and activated with $ZnCl_2$ to study the structural stability of the molecules. We determine the equilibrium pressure by means of adsorption isotherms and the van't Hoff equation, which suggests that Ca-decorated carbyne could operate as hydrogen storage media at temperatures above the boiling temperature of liquid nitrogen presented in this work.

CONCLUSIONS

We performed the analysis of activated carbyne C_{12}-ring with zinc dichloride ($ZnCl_2$) and decorated it with Ca atoms by DFT calculations. First, the pristine carbyne C_{12}-ring used in this work corresponds to the C_{4N} structure with $N = 3$, with a $D_{(n/2)h}$ symmetry. The pristine C_{12}-ring exhibits area and pore diameter of 18.37 $Å^2$ and 4.83 Å, respectively. According to this, our results using activated carbyne C_{12}-ring show an increase in area and pore diameter of 5.17% and 2.69%, respectively. In the case of several carbon-based nanomaterials, the hydrogen adsorption on pristine carbyne is impractical due to weak interactions of H_2 molecules on the host material, since the adsorption energies of a single H_2 molecule at the outer and inner surfaces of pristine carbyne are only 0.077 eV per H_2 and 0.028 eV per H_2, respectively. In order, to increase the hydrogen storage properties on pristine C_{12}-ring, we activate the ring through chemical activation with zinc dichloride ($ZnCl_2$) to increase the surface area and enhance pore size distribution. These theoretical specific surface area on activated carbyne results in an increase from ∼4606.31 $m^2\ g^{-1}$ (pristine C_{12}-ring) to ∼4844.33 $m^2\ g^{-1}$. The accessible surface area shows a value of 13000 $m^2\ g^{-1}$ for pristine carbyne, whereas activated carbyne shows a value of 15045.88 $m^2\ g^{-1}$, which shows an increase of 15.76% with respect to that of the pure carbyne. These values represent a macroscopic parameter that can be helpful to adjust the synthesis condition of the carbyne molecule. Unlike pristine C_{12}-ring, the activated ring can adsorb two H_2 molecules at the center of the molecule with a desirable binding energy of ∼0.1 eV per H_2. However, the hydrogen storage capacity obtained is only 2.72 wt % which does not fulfill objectives established by the DOE. Subsequently, we studied the case of a single Ca atom adsorbed on a carbyne surface (outer and inner), and we calculate the binding energy of the CaC_{12} system, showing values of 2.79 eV for single and triple bond zones, where Ca atom was placed, and of 3.34 eV for the center of the activated ring, which represents an increase of 49.77% with respect to the pristine carbyne. In addition, we determine the zones that Ca atoms prefer to bind on the carbyne molecule (in front of single and triple bonds and the center of the ring), which makes it more attractive in comparison with pristine C_{12}-ring, which only has an area for placement of the calcium atom in front of single bonds of the ring. The activation of the carbyne ring produces higher stability on the ring, causing more Ca atoms that can bind to the host material. We showed that Ca adatoms at small concentrations stay atomically dispersed on carbyne, donating +0.94e and +1.05e to the ring, for Mulliken population analysis and ESP-fitted charges, respectively. Furthermore, in the presence of Ca, hydrogen adsorption increases 21.8% in comparison with Ca-decorated pristine carbyne. We determine that up to seven H_2 molecules can be physically adsorbed with an average energy of ∼0.39 eV per H_2 molecule. The first six H_2 molecules tend to adsorb around the Ca atom and the seventh H_2 molecule is adsorbed on the top of the Ca atom. The hydrogen storage capacity obtained in this study is 7.11 wt % and therefore represents an increase of 15% with respect to the pristine carbyne. However, it is expected to reach 13.8 wt % with three Ca atoms, which represents an increase of 124% with respect to pristine carbyne, and satisfactorily meets the target set by the DOE for the year 2025. We determine the equilibrium pressure for CaC_{12}−$7H_2$ and Ca_3C_{12}−$21H_2$ systems (5−15 MPa), by isotherm calculations. Furthermore, the T_D, which is calculated using the van't Hoff equation, suggests that Ca-decorated carbyne could operate as hydrogen storage media at temperatures above the boiling temperature of liquid nitrogen. The molecular dynamics after 6 ps at 300 K show unified thermal stability when the Nosé−Hoover thermostat was used. The average temperatures were 300.94 and 300.23 K for CaC_{12}−$7H_2$ (pristine and activated carbyne). For doped complex Ca_3C_{12}−$21H_2$, the average temperature was 301.44 K with the Nosé−Hoover thermostat. Every system was equilibrated for 3−6 ps, and after 6 ps of production, no breaking of bonds was observed, which implied the thermal stability of the systems. Therefore, the activated carbyne decorated with Ca atoms attains H_2 storage capacity which is much higher than other carbon and carbon-based materials reported in the literature (see Table 2), fulfilling DOE requirements, so this material certainly requires further experimental investigation.

https://doi.org/10.1021/acsomega.1c06149
ACS Omega 2022, 7, 10100−10114

COMPUTATIONAL METHODS

Density functional theory calculations are carried out to activate carbyne C_{12}-ring through chemical activation with zinc dichloride ($ZnCl_2$), and decorating with Ca atoms, by means of Biovia Materials Studio Dmol^3 software[57,58] to determine its capability of hydrogen storage. To calculate adsorption energies, the generalized gradient approximation (GGA) with Perdew−Burke−Ernzerhof (PBE) functional[59] and spin unrestricted was used. The interaction energies between hydrogen molecules with one C_{12}-ring are calculated by means of a set of double numerical plus polarization basis (DNP). For occupied orbital, we consider two atomic orbitals in the basis set. For C and H atoms, d- and p-polarization functions are respectively used. The employed basis set has the advantage of being equivalent to the analytical basis set 6-31G**. All presented geometry optimizations are obtained for a tolerance on which the maximum forces are lower than 0.002 Ha/Å. Here the effect of van der Waals interactions is included explicitly by using the empirical correction scheme of Grimme (DFT-D) for periodic systems.[60] Standard values of the dispersion coefficients C_6 (0.14, 1.75, and 10.80 J nm^6 mol^{-1}, for H, C, and Ca, respectively), vdW radii (1.001, 1.452, and 1.474 Å), cutoff radius for pair interactions (30.0 Å), PBE global scaling factor S_6 (0.75), and damping factor d (20.0) have been used. In addition, the total energies, HOMO−LUMO, electronic charge density, Mulliken population analysis, and electrostatic potential fitting charges are calculated. Sorption Monte Carlo simulations of BIOVIA Materials Studio using Compass Force field and Metropolis method have been applied on a cell (15 Å per side and 90° per angle) containing our molecular hydrogen adsorbed on carbyne doped with calcium with the aim to build logarithmic adsorption isotherms.

ASSOCIATED CONTENT

Supporting Information

The Supporting Information is available free of charge at https://pubs.acs.org/doi/10.1021/acsomega.1c06149.

DFT-based MD simulations and mean square displacements with Nosé−Hoover thermostat (Figures S1−S6); Mulliken population analysis and (ESP)-fitted charges (Table S1) (PDF)

AUTHOR INFORMATION

Corresponding Author

Luis Alberto Desales Guzmán − *División de Estudios de Posgrado e Investigación, Instituto Tecnológico de Toluca, Metepec 52149 Estado de México, México;* orcid.org/0000-0003-3149-4624; Phone: 527292804328; Email: ldesalesg@toluca.tecnm.mx

Authors

Juan Horacio Pacheco Sánchez − *División de Estudios de Posgrado e Investigación, Instituto Tecnológico de Toluca, Metepec 52149 Estado de México, México;* orcid.org/0000-0002-9525-5473

Juan Salvador Arellano Peraza − *Área de Física Atómica Molecular Aplicada, Universidad Autónoma Metropolitana Azcapotzalco, C.P. 02200 Ciudad de México, México*

Complete contact information is available at: https://pubs.acs.org/10.1021/acsomega.1c06149

Notes

The authors declare no competing financial interest.

ACKNOWLEDGMENTS

We express our sincere gratitude to TecNM-Instituto Tecnológico de Toluca, for the facilities to develop the research. Finally, we thank the Consejo Mexiquense de Ciencia y Tecnología (COMECYT) for the grant awarded and the UAM-Azcapotzalco for the collaboration on this paper. Thanks to all those mentioned because without their support this work would not have been possible to carry out.

REFERENCES

(1) Sevilla, M.; Mokaya, R. Energy Storage Applications of Activated Carbons: Supercapacitors and Hydrogen Storage. *Energy Environ. Sci.* **2014**, *7* (4), 1250−1280.

(2) Si, L.; Tang, C. The Reversible Hydrogen Storage Abilities of Metal Na (Li, K, Ca, Mg, Sc, Ti, Y) Decorated All-Boron Cage B28. *Int. J. Hydrogen Energy* **2017**, *42* (26), 16611−16619.

(3) Beheshti, E.; Nojeh, A.; Servati, P. A First-Principles Study of Calcium-Decorated, Boron-Doped Graphene for High Capacity Hydrogen Storage. *Carbon* **2011**, *49* (5), 1561−1567.

(4) Li, C.; Li, J.; Wu, F.; Li, S.-S.; Xia, J.-B.; Wang, L.-W. High Capacity Hydrogen Storage in Ca Decorated Graphyne: A First-Principles Study. *J. Phys. Chem. C* **2011**, *115* (46), 23221−23225.

(5) *DOE Technical Targets for Onboard Hydrogen Storage for Light-Duty Vehicles* |; U.S. Department of Energy; https://www.energy.gov/eere/fuelcells/doe-technical-targets-onboard-hydrogen-storage-light-duty-vehicles (accessed 2021-06-25).

(6) Blackman, J. M.; Patrick, J. W.; Arenillas, A.; Shi, W.; Snape, C. E. Activation of Carbon Nanofibres for Hydrogen Storage. *Carbon* **2006**, *44* (8), 1376−1385.

(7) Jordá-Beneyto, M.; Suárez-García, F.; Lozano-Castelló, D.; Cazorla-Amorós, D.; Linares-Solano, A. Hydrogen Storage on Chemically Activated Carbons and Carbon Nanomaterials at High Pressures. *Carbon* **2007**, *45* (2), 293−303.

(8) Ströbel, R.; Garche, J.; Moseley, P. T.; Jörissen, L.; Wolf, G. Hydrogen Storage by Carbon Materials. *J. Power Sources* **2006**, *159* (2), 781−801.

(9) Schur, D.V.; Tarasov, B.P.; Yu. Zaginaichenko, S.; Pishuk, V.K.; Veziroglu, T.N.; Shul'ga, Y. M.; Dubovoi, A.G.; Anikina, N.S.; Pomytkin, A.P.; Zolotarenko, A.D. The Prospects for Using of Carbon Nanomaterials as Hydrogen Storage Systems. *Int. J. Hydrogen Energy* **2002**, *27* (10), 1063−1069.

(10) Nechaev, Y. S. Carbon Nanomaterials, Relevance to Solving the Hydrogen Storage Problem. *J. Nano Res.* **2010**, *12*, 1−44.

(11) Patchkovskii, S.; Tse, J. S.; Yurchenko, S. N.; Zhechkov, L.; Heine, T.; Seifert, G. From The Cover: Graphene Nanostructures as Tunable Storage Media for Molecular Hydrogen. *Proc. Natl. Acad. Sci. U. S. A.* **2005**, *102* (30), 10439−10444.

(12) Liu, C.; Chen, Y.; Wu, C. Z.; Xu, S. T.; Cheng, H. M. Hydrogen Storage in Carbon Nanotubes Revisited. *Carbon* **2010**, *48* (2), 452−455.

(13) Pupysheva, O. V.; Farajian, A. A.; Yakobson, B. I. Fullerene Nanocage Capacity for Hydrogen Storage. *Nano Lett.* **2008**, *8* (3), 767−774.

(14) Anikina, E.; Banerjee, A.; Beskachko, V.; Ahuja, R. Li-Decorated Carbyne for Hydrogen Storage: Charge Induced Polarization and van't Hoff Hydrogen Desorption Temperature. *Sustainable Energy Fuels* **2020**, *4* (2), 691−699.

(15) Antipina, L. Y.; Avramov, P. V.; Sakai, S.; Naramoto, H.; Ohtomo, M.; Entani, S.; Matsumoto, Y.; Sorokin, P. B. High Hydrogen-Adsorption-Rate Material Based on Graphane Decorated with Alkali Metals. *Phys. Rev. B* **2012**, *86* (8), 85435.

(16) Yoon, M.; Yang, S.; Hicke, C.; Wang, E.; Geohegan, D.; Zhang, Z. Calcium as the Superior Coating Metal in Functionalization of Carbon Fullerenes for High-Capacity Hydrogen Storage. *Phys. Rev. Lett.* **2008**, *100* (20), 1−4.

(17) Lee, H.; Ihm, J.; Cohen, M. L.; Louie, S. G. Calcium-Decorated Carbon Nanotubes for High-Capacity Hydrogen Storage: First-Principles Calculations. *Phys. Rev. B: Condens. Matter Mater. Phys.* **2009**, *80* (11), 1−5.
(18) Sorokin, P. B.; Lee, H.; Antipina, L. Y.; Singh, A. K.; Yakobson, B. I. Calcium-Decorated Carbyne Networks as Hydrogen Storage Media. *Nano Lett.* **2011**, *11* (7), 2660−2665.
(19) Wu, G.; Wang, J.; Zhang, X.; Zhu, L. Hydrogen Storage on Metal-Coated B80 Buckyballs with Density Functional Theory. *J. Phys. Chem. C* **2009**, *113* (17), 7052−7057.
(20) Er, S.; De Wijs, G. A.; Brocks, G. Improved Hydrogen Storage in Ca-Decorated Boron Heterofullerenes : A Theoretical Study. *J. Mater. Chem. A* **2015**, *3*, 7710−7714.
(21) Desales-Guzmán, L. A.; Pacheco-Sánchez, J. H.; García-Rosales, G.; Isidro-Ortega, F. J. Modelling Carbyne C12-Ring Calcium Decorated for Hydrogen Storage. *Rev. Mex. Fis.* **2018**, *64* (6), 634−641.
(22) Wang, J.; Du, Y.; Sun, L. Ca-Decorated Novel Boron Sheet: A Potential Hydrogen Storage Medium. *Int. J. Hydrogen Energy* **2016**, *41* (10), 5276−5283.
(23) Ataca, C.; Aktürk, E.; Ciraci, S. Hydrogen Storage of Calcium Atoms Adsorbed on Graphene: First-Principles Plane Wave Calculations. *Phys. Rev. B: Condens. Matter Mater. Phys.* **2009**, *79* (4), 1−4.
(24) Desales-Guzmán, L. A.; Pacheco-Sánchez, J. H.; Isidro-Ortega, F. J.; De la Mora-Zarco, K. Hydrogen Storage in Ca-Decorated Carbyne C10-Ring on Either Dnh or D(n/2)h Symmetry. DFT Study. *Int. J. Hydrogen Energy* **2020**, *45* (11), 6780−6792.
(25) Casari, C. S.; Milani, A. Carbyne: From the Elusive Allotrope to Stable Carbon Atom Wires. *MRS Commun.* **2018**, *8*, 207−219.
(26) Banhart, F. Chains of Carbon Atoms : A Vision or a New Nanomaterial ? *Beilstein J. Nanotechnol.* **2015**, *6*, 559−569.
(27) Eisler, S.; Slepkov, A. D.; Elliott, E.; Luu, T.; McDonald, R.; Hegmann, F. A.; Tykwinski, R. R. Polyynes as a Model for Carbyne: Synthesis, Physical Properties, and Nonlinear Optical Response. *J. Am. Chem. Soc.* **2005**, *127* (8), 2666−2676.
(28) Liu, M.; Yakobson, B. I.; Lee, H.; Artyukhov, V. I.; Xu, F. Correction to Carbyne from First-Principles: Chain of C Atoms, a Nanorod or a Nanorope. *ACS Nano* **2017**, *11* (5), 5186−5186.
(29) Tommasini, M.; Milani, A.; Fazzi, D.; Lucotti, A.; Castiglioni, C.; Januszewski, J. A.; Wendinger, D.; Tykwinski, R. R. π-Conjugation and End Group Effects in Long Cumulenes: Raman Spectroscopy and DFT Calculations. *J. Phys. Chem. C* **2014**, *118* (45), 26415−26425.
(30) Januszewski, J. A.; Tykwinski, R. R. Synthesis and Properties of Long [n]Cumulenes ($n \geq 5$). *Chem. Soc. Rev.* **2014**, *43* (9), 3184−3203.
(31) Remya, K.; Suresh, C. H. Carbon Rings: A DFT Study on Geometry, Aromaticity, Intermolecular Carbon-Carbon Interactions and Stability. *RSC Adv.* **2016**, *6* (50), 44261−44271.
(32) Torelli, T.; Mitas, L. Electron Correlation in C4N+2 Carbon Rings: Aromatic versus Dimerized Structures. *Phys. Rev. Lett.* **2000**, *85*, 1702−1705.
(33) González-García, P. Activated Carbon from Lignocellulosics Precursors: A Review of the Synthesis Methods, Characterization Techniques and Applications. *Renewable Sustainable Energy Rev.* **2018**, *82*, 1393−1414.
(34) Sethia, G.; Sayari, A. Activated Carbon with Optimum Pore Size Distribution for Hydrogen Storage. *Carbon* **2016**, *99*, 289−294.
(35) Marsh, H.; Rodríguez-Reinoso, F. Characterization of Activated Carbon. *Activated Carbon*, 1st ed.; Elsevier Science & Technology Books, 2006; Chapter 4. DOI: 10.1016/B978-008044463-5/50018-2.
(36) Yushin, G.; Dash, R.; Jagiello, J.; Fischer, J. E.; Gogotsi, Y. Carbide-Derived Carbons: Effect of Pore Size on Hydrogen Uptake and Heat of Adsorption. *Adv. Funct. Mater.* **2006**, *16* (17), 2288−2293.
(37) Zhang, C.; Geng, Z.; Cai, M.; Zhang, J.; Liu, X.; Xin, H.; Ma, J. Microstructure Regulation of Super Activated Carbon from Biomass Source Corncob with Enhanced Hydrogen Uptake. *Int. J. Hydrogen Energy* **2013**, *38* (22), 9243−9250.
(38) Monteiro de Castro, M.; Martínez-Escandell, M.; Molina-Sabio, M.; Rodríguez-Reinoso, F. Hydrogen Adsorption on KOH Activated Carbons from Mesophase Pitch Containing Si, B, Ti or Fe. *Carbon* **2010**, *48* (3), 636−644.
(39) Arami-Niya, A.; Daud, W. M. A. W.; Mjalli, F. S. Using Granular Activated Carbon Prepared from Oil Palm Shell by ZnCl 2 and Physical Activation for Methane Adsorption. *J. Anal. Appl. Pyrolysis* **2010**, *89* (2), 197−203.
(40) Boonpoke, A.; Chiarakorn, S.; Laosiripojana, N.; Towprayoon, S.; Chidthaisong, A. Synthesis of Activated Carbon and MCM-41 from Bagasse and Rice Husk and Their Carbon Dioxide Adsorption Capacity. *J. Sustain. Energy Environ.* **2011**, *2*, 77−81.
(41) Wang, J.; Kaskel, S. KOH Activation of Carbon-Based Materials for Energy Storage. *J. Mater. Chem.* **2012**, *22* (45), 23710.
(42) Hu, Y. H. Stability of Sp Carbon (Carbyne) Chains. *Phys. Lett. Sect. A Gen. At. Solid State Phys.* **2009**, *373* (39), 3554−3557.
(43) Peigney, A.; Laurent, C.; Flahaut, E.; Bacsa, R. R.; Rousset, A. Specific Surface Area of Carbon Nanotubes and Bundles of Carbon Nanotubes. *Carbon N. Y.* **2001**, *39* (4), 507−514.
(44) Frost, H.; Düren, T.; Snurr, R. Q. Effects of Surface Area, Free Volume, and Heat of Adsorption on Hydrogen Uptake in Metal-Organic Frameworks. *J. Phys. Chem. B* **2006**, *110* (19), 9565−9570.
(45) Pacheco-Sánchez, J. H.; Zaragoza Rivera, I. P.; Bravo Ortega, A. Interaction of Small Carbon Molecules and Zinc Dichloride : DFT Study. *Rev. Mex. Fis.* **2017**, *63*, 97−110.
(46) Cruz-Torres, A.; Castillo Alvarado, F. de L.; Ortiz-Lopez, J.; Arellano, J. S. Hydrogen Storage Inside a Toroidal Carbon Nanostructure C120: Density Functional Theory Computer Simulation. *Int. J. Quantum Chem.* **2010**, *110*, 2495−2508.
(47) Atkins, P.; De Paula, J. *Physical Chemistry*, 8th ed.; W. H. Freeman, 2006.
(48) Isidro-Ortega, F. J.; Pacheco-Sánchez, J. H.; Desales-Guzmán, L. A. Hydrogen Storage on Lithium Decorated Zeolite Templated Carbon, DFT Study. *Int. J. Hydrogen Energy* **2017**, *42* (52), 30704−30717.
(49) Windiks, R.; Delley, B. Massive Thermostatting in Isothermal Density Functional Molecular Dynamics Simulations. *J. Chem. Phys.* **2003**, *119* (5), 2481−2487.
(50) Kassir, Y.; Kupiec, M.; Shalom, A.; Simchen, G. Cloning and Mapping of CDC40, a Saccharomyces Cerevisiae Gene with a Role in DNA Repair. *Curr. Genet.* **1985**, *9* (4), 253−257.
(51) Tuckerman, M.; Berne, B. J.; Martyna, G. J. Reversible Multiple Time Scale Molecular Dynamics. *J. Chem. Phys.* **1992**, *97* (3), 1990−2001.
(52) Kubas, G. J. Metal-Dihydrogen and σ-Bond Coordination: The Consummate Extension of the Dewar-Chatt-Duncanson Model for Metal-Olefin π Bonding. *J. Organomet. Chem.* **2001**, *635* (1−2), 37−68.
(53) Babeł, K.; Jurewicz, K. KOH Activated Lignin Based Nanostructured Carbon Exhibiting High Hydrogen Electrosorption. *Carbon* **2008**, *46* (14), 1948−1956.
(54) Vargas, D. P.; Giraldo, L.; Erto, A.; Moreno-Piraján, J. C. Chemical Modification of Activated Carbon Monoliths for CO2 Adsorption. *J. Therm. Anal. Calorim.* **2013**, *114* (3), 1039−1047.
(55) Zhou, C.; Szpunar, J. A. Hydrogen Storage Performance in Pd/Graphene Nanocomposites. *ACS Appl. Mater. Interfaces* **2016**, *8* (39), 25933−25940.
(56) Isidro-Ortega, F. J.; Pacheco-Sánchez, J. H.; Alejo, R.; Desales-Guzmán, L. A.; Arellano, J. S. Theoretical Studies in the Stability of Vacancies in Zeolite Templated Carbon for Hydrogen Storage. *Int. J. Hydrogen Energy* **2019**, *44* (13), 6437−6447.
(57) Delley, B. An All-Electron Numerical Method for Solving the Local Density Functional for Polyatomic Molecules. *J. Chem. Phys.* **1990**, *92* (1), 508−517.
(58) Delley, B. From Molecules to Solids with the DMol3 Approach. *J. Chem. Phys.* **2000**, *113* (18), 7756−7764.
(59) Perdew, J. P.; Burke, K.; Ernzerhof, M. Generalized Gradient Approximation Made Simple. *Phys. Rev. Lett.* **1996**, *77* (18), 3865−3868.
(60) Grimme, S. Semiempirical GGA-Type Density Functional Constructed with a Long-Range Dispersion Correction. *J. Comput. Chem.* **2006**, *27* (15), 1787−1799.

https://doi.org/10.1021/acsomega.1c06149
ACS Omega 2022, 7, 10100−10114